

Molecule opacity study on low-lying states of CS

Rui Li(李瑞), Jiqun Sang(桑纪群), Xiaohe Lin(林晓贺), Jianjun Li(李建军), Guiying Liang(梁桂颖), and Yong Wu(吴勇)

Citation: Chin. Phys. B, 2022, 31 (**10**): 103101. DOI: 10.1088/1674-1056/ac834f
Journal homepage: http://cpb.iphy.ac.cn; http://iopscience.iop.org/cpb

What follows is a list of articles you may be interested in

Relativistic calculations on the transition electric dipole moments and radiative lifetimes of the spin-forbidden transitions in the antimony hydride molecule

Yong Liu(刘勇), Lu-Lu Li(李露露), Li-Dan Xiao(肖利丹), and Bing Yan(闫冰)
Chin. Phys. B, 2022, 31 (**8**): 083101. DOI: 10.1088/1674-1056/ac6ee1

Theoretical study on the transition properties of AlF

Yun-Guang Zhang(张云光), Ling-Ling Ji(吉玲玲), Ru Cai(蔡茹),Cong-Ying Zhang(张聪颖), and Jian-Gang Xu(徐建刚)
Chin. Phys. B, 2022, 31 (**5**): 053101. DOI: 10.1088/1674-1056/ac3648

Configuration interaction study on low-lying states of AlCl molecule

Xiao-Ying Ren(任笑影), Zhi-Yu Xiao(肖志宇), Yong Liu(刘勇), and Bing Yan(闫冰)
Chin. Phys. B, 2021, 30 (**5**): 053101. DOI: 10.1088/1674-1056/abd46a

Vibronic spectra of aluminium monochloride relevant to circumstellar molecule

Jian-Gang Xu(徐建刚), Cong-Ying Zhang(张聪颖), Yun-Guang Zhang(张云光)
Chin. Phys. B, 2020, 29 (**3**): 033102. DOI: 10.1088/1674-1056/ab6c46

Molecular opacities of low-lying states of oxygen molecule

Gui-Ying Liang(梁桂颖), Yi-Geng Peng(彭裔耕), Rui Li(李瑞), Yong Wu(吴勇), Jian-Guo Wang(王建国)
Chin. Phys. B, 2020, 29 (**2**): 023101. DOI: 10.1088/1674-1056/ab5fb6

Molecule opacity study on low-lying states of CS

Rui Li(李瑞)[1,2], Jiqun Sang(桑纪群)[1], Xiaohe Lin(林晓贺)[3,2,†], Jianjun Li(李建军)[1], Guiying Liang(梁桂颖)[4], and Yong Wu(吴勇)[2,5,‡]

[1] *Department of Physics, College of Science, Qiqihar University, Qiqihar* 161006, *China*
[2] *National Key Laboratory of Computational Physics, Institute of Applied Physics and Computational Mathematics, Beijing* 100088, *China*
[3] *Faculty of Foundation, Space Engineering University, Beijing* 101416, *China*
[4] *School of Data Science and Artificial Intelligence, Jilin Engineering Normal University, Changchun* 130052, *China*
[5] *HEDPS, Center for Applied Physics and Technology, Peking University, Beijing* 100084, *China*

(Received 17 June 2022; revised manuscript received 21 July 2022; accepted manuscript online 22 July 2022)

CS molecule, which plays a key role in atmospheric and astrophysical circumstances, has drawn great attention for long time. Owing to its large state density, the detailed information of the electronic structure of CS is still lacking. In this work, the high-level MRCI+Q method is used to compute the potential energy curves, dipole moments and transition dipole moments of singlet and triplet states correlated with the lowest dissociation limit of CS, based on which high accurate vibration–rotation levels and spectroscopic constants of bound states are evaluated. The opacity of CS relevant to atmospheric circumstance is computed at a pressure of 100 atms for different temperatures. With the increase of temperature, band systems from different transitions mingle with each other, and band boundaries become blurred, which are originated from the increased population on vibrational excited states and electronic excited states at high temperature.

Keywords: CS, transition dipole moment, opacity, excited state

PACS: 31.50.Df, 31.15.ag, 31.15.aj **DOI:** 10.1088/1674-1056/ac834f

1. Introduction

The CS molecule is of great interest since it plays a key role in atmospheric and astrophysical circumstances, which draws great attention from researchers.[1–5] The molecule has been detected in the diffuse clouds, dense clouds, molecular clouds, interstellar clouds, comets, carbon-rich stars and other galaxies. In the atmospheric and astrophysical investigations, the opacity between low-lying states are used to determine species, isotopic abundances and number densities in the environment. Thereby, spectroscopic properties of CS provide worthwhile information to an extensive understanding for the intermediate processes occurred in the upper atmosphere. CS molecule and sulfur-containing molecules in the stratosphere are also related to formation of sulfate aerosols, which may lead to acid rain effect and global climate change.[6] Hence, electronic structure and transition properties of the CS molecule have been continually arising interest in the past several decades.

The large numbers of astronomical detections of CS and the key role in the Earth's atmosphere have motivated a great deal of experimental studies. In experiment, the wavelength region of CS ranges from the microwave to ultraviolet (UV). In 1934, the pioneer work of main $A^1\Pi$–$X^1\Sigma^+$ transition was performed by Crawford *et al.*[7] Later, the rotational spectrum of CS was firstly detected by Mockler and Bird.[8] The rotational spectrum of CS was also photographed by Lovas and Krupenie, and dipole moments and rotational constants were fitted by experimental results.[9] The experimental spectrum in the millimeter region was observed by Bogey *et al.*,[10,11] and the spectroscopic constants of the $X^1\Sigma^+$ state were obtained. More recently, the investigation in the wide wavelength region was extensively studied by Kim *et al.*[12] and Gottlieb *et al.*,[13] and the accurate frequencies of rotational transitions were provided in their studies.

The first work in the infra-red wavelengths was carried out by Todd,[14] who detected the $v = 2$–0 vibration–rotation band of the $X^1\Sigma^+$ state of CS. Subsequently, the investigation of the infra-red region was extended by Winkel *et al.*[15] and Burkholder *et al.*,[16] and high resolution of the $v = 1$–0 absorption band and the $v = 1$–0 "hot" band for the $X^1\Sigma^+$ state were measured. On the basis of vibration–rotation and pure rotation spectrum in preceding experimental data, Conxon and Hajigeorgiou determined accurate spectroscopic potential energy curve (PEC). Then, the spectroscopic constant of the $X^1\Sigma^+$ state was improved by Ram *et al.*,[17] who determined the spectroscopic constant from $\Delta v = 1$ vibration–rotation bands up to $v = 9$–8. Recently, Uehara *et al.*[2] measured $\Delta v = 1$ transitions of the $X^1\Sigma^+$ state with $v \leq 7$ to a better precision than Ram *et al.* Paulose *et al.*[1] used the spectroscopically-determined PEC and dipole moment to present vibration–rotation line lists.

A series of UV band ($A^1\Pi$–$X^1\Sigma^+$, $A'^1\Sigma^+$–$X^1\Sigma^+$, $a^3\Pi$–$X^1\Sigma^+$, and so on) were extensively studied by different research groups. Bergeman and Cossart[18,19] observed a number of spin-allowed ($A^1\Pi$–$X^1\Sigma^+$) and spin-forbidden ($a^3\Pi$–

†Corresponding author. E-mail: xiaohelin1989@163.com
‡Corresponding author. E-mail: wu_yong@iapcm.ac.cn

© 2022 Chinese Physical Society and IOP Publishing Ltd

$X^1\Sigma^+$, $d^3\Delta$–$X^1\Sigma^+$, and $e^3\Sigma^-$–$X^1\Sigma^+$) transition bands, and the interaction between those low-lying excited states were discussed in detail. The $A^1\Pi$–$X^1\Sigma^+$ band system was recorded by Mahon *et al.*,[20] and electronic transition moment of the $A^1\Pi$–$X^1\Sigma^+$ transition were estimated by the corresponding experimental result. The emission spectrum of $A'^1\Sigma^+$–$X^1\Sigma^+$ was photographed by Dornhöfer *et al.*[21] employing time-resolved fluorescence technique, and the transition property of $A'^1\Sigma^+$–$X^1\Sigma^+$ was analyzed.

On the theoretical side, the electronic structure and transition properties of CS have been investigated by different theoretical method. Robbe and Schamps[22] used SCF-CI approach to calculated electronic structure, wavefunction and dipole moment of valence state of CS. Later, the PEC of $X^1\Sigma^+$ state were determined by Wilson[23] by using diagrammatic many-body perturbation theory. Ornellas[24] determined accurate PECs of $X^1\Sigma^+$ and $A^1\Pi$ states by utilizing MRCI method, and the transition dipole moment of the $A^1\Pi$–$X^1\Sigma^+$ transition were evaluated. The structures for triplet states ($a^3\Pi$, $d^3\Delta$, $a'^3\Sigma^+$ and $e^3\Sigma^-$) were studied by Hochlaf using CASSCF and MRCI method.[25]

As discussed above, the CS molecule has been studied widely by different research group. However, the existing computations of CS molecule are dominantly concentrated on structures of several electronic states. Regarding the large state density and interaction of low-lying states, the accurate calculations of electronic structure and spectroscopic properties of CS still remain sparse. As far as we know, the only spectrum simulation is the vibration–rotation line lists computations of the $X^1\Sigma^+$ state of CS by Paulose *et al.*[1] In this work, we carry out high-level MRCI study on the low-lying states of CS. The PECs, dipole moments and transition dipole moments are evaluated at the MRCI level of theory, and then vibration–rotation line between low-lying states are calculated at different temperature conditions.

2. Theoretical method

In the present work, the MOLPRO package[26] is used to calculate the PECs of singlet and triplet states correlated with the lowest dissociation limit of CS molecule. All the calculations are done in the C_{2v} group, which is subgroup of $C_{\infty v}$ point group for CS molecule. The corresponding relationship for the irreducible representations of C_{2v} and $C_{\infty v}$ group are Σ^+ to A_1, Σ^- to A_2, Π to B_1+B_2 and Δ to A_1+A_2. For the C and S atoms, the contracted augmented correlation-consistent polarized quintuple zeta aug-cc-pwCV5Z-DK basis sets[27–29] is adopted. Within the internuclear distance range of 0.975–6.0 Å, the molecular orbitals of the $X^1\Sigma^+$ state are computed by the Hartree–Fock approach. In order to balance molecular orbitals applied in the subsequent calculations of electronic correlation, we utilize the state-averaged complete active space self-consistent field (SA-CASSCF)[30,31] approach to optimize the preceding Hartree–Fock molecular orbitals. In the SA-CASSCF calculations, all the 12 singlet and triplet Λ–S states, which are two $^1\Sigma^+$, one $^1\Sigma^-$, two $^1\Pi$, one $^1\Delta$, two $^3\Sigma^+$, one $^3\Sigma^-$, two $^3\Pi$ and one $^3\Delta$, are taken into account simultaneously. The active space in the SA-CASSCF calculations is constructed by 8 molecular orbitals, which associates with C 2s2p and S 3s3p atomic orbitals. In the C_{2v} group, the active space is denoted as (4,2,2,0), in which ten electrons are spread across 8 molecular orbitals. Subsequently, by employing the calculated CASSCF energies as reference values, the energies of the 12Λ–S states are determined by internally contracted multireference configuration interaction method[32,33] (MRCI+Q) (including Davison size-extensivity correction).[34] The scalar relativistic effect is taken into account through third-order Douglas–Kroll and Hess integrals.[35,36] The PECs are presented by linking the energy points of Λ–S states via taking into account the non-crossing rule.

Under the Born–Oppenheimer approximation condition, the electronic Schrödinger equation of diatomic molecules can be written as

$$\hat{H}_e \Psi_e(r,R) = E_e(R)\Psi_e(r,R), \tag{1}$$

in which $\hat{H}_e$ is Hamiltonian of the N electrons of diatomic molecules, $\Psi_e(r,R)$ and $E_e(R)$ are the eigen-function and eigen-energy, respectively.

$$\hat{H}_e = \sum_{i=1}^{N}\left(-\frac{1}{2}\nabla_i^2\right) + \sum_{i=1}^{N}\left(-\frac{Z_a}{r_{ai}} - \frac{Z_b}{r_{bi}}\right) + \sum_{i<j=1}^{N}\left(\frac{1}{r_{ij}}\right) + \frac{Z_a Z_b}{R}, \tag{2}$$

where Z_a and Z_b are the charge number of nucleus A and B.

On the basis of calculated energies of electronic states, the eigenvalues and wave functions of vibration–rotation states can be obtained by solution of radical nuclear Schrödinger equation

$$\left[-\frac{1}{2\mu}\frac{d^2}{dR^2} + E_e(R)\right]\chi_{vJ}(R) = E_{vJ}\chi_{vJ}(R) \tag{3}$$

in which $E_{vJ}(R)$is vibration–rotation level.

$$A_{v'j',v''j''} = \frac{4}{3}\alpha^3\omega^3_{v'j',v''j''}\frac{S_{J'J''}}{2J''+1} \tag{4}$$

in which

$$S_{J'J''} = |\langle\chi_{v'J'}|D(R)|\chi_{v''J''}\rangle|^2\varphi_{J'J''}, \tag{5}$$

where v' and J' are vibrational and rotational quantum numbers, α is fine-structure constant, $\omega_{v'j',v''j''}$ is transition frequency between different vibration–rotation levels, $S_{J'J''}$ is the line strength, $D(R)$ is the transition dipole moment, and $\varphi_{J',J''}$ is Hönl–London factor. The Hönl–London factor $\varphi_{J'J''}$ is defined as

$$\varphi_{J',J''}=\begin{cases}\Delta\Lambda=0, \dfrac{(J''+\Lambda'')(J''-\Lambda'')}{J''},\\ \Delta\Lambda=+1, \dfrac{(J''-1-\Lambda'')(J''-\Lambda'')}{4J''}, \quad (P\text{-branch}),\\ \Delta\Lambda=-1, \dfrac{(J''-1+\Lambda'')(J''+\Lambda'')}{4J''},\end{cases}$$

$$\varphi_{J',J''}=\begin{cases}\Delta\Lambda=0, \dfrac{(2J''+1)^2\Lambda''^2}{J''(J''+1)},\\ \Delta\Lambda=+1, \dfrac{(J''+1+\Lambda'')(J''-\Lambda'')(2J''+1)}{4J''(J''+1)}, \quad (Q\text{-branch}),\\ \Delta\Lambda=-1, \dfrac{(J''+1-\Lambda'')(J''+\Lambda'')(2J''+1)}{4J''(J''+1)},\end{cases}$$

$$\varphi_{J',J''}=\begin{cases}\Delta\Lambda=0, \dfrac{(J''+1+\Lambda'')(J''+1-\Lambda'')}{J''+1},\\ \Delta\Lambda=+1, \dfrac{(J''+2+\Lambda'')(J''+1+\Lambda'')}{4(J''+1)}, \quad (R\text{-branch}).\\ \Delta\Lambda=-1, \dfrac{(J''+2-\Lambda'')(J''+1-\Lambda'')}{4(J''+1)},\end{cases} \tag{6}$$

The expressions of formulas (1–6) can be found in Ref. [36].

Molecular opacity is computed with integrated line strengths,[37] which is given by

$$\sigma=\frac{1}{8\pi(\Delta E''/hc)^2}\times\frac{A(2J'+1)\exp(-E_{V'J',00}hc/kT)[1-\exp(-\Delta E''/kT]}{Q}, \tag{7}$$

in which Einstein's coefficients A is obtained from Eq. (4), $\Delta E''$ is the energy gap of the correlated two states, h is the Plank constant, c is the speed of light in vacuum, k is the Boltzmann constant, $E_{V'J',00}$ is the excitation energy of the lower state in cm^{-1}, and the total internal partition function $Q(T)$ is defined by summing up concerned electronic state weighed by the Boltzmann factor utilizing

$$Q=\sum_{i=1}^{n}Q_{ei}Q_{vi}Q_{ri}\exp\left(-\frac{T_i hc}{kT}\right), \tag{8}$$

where T is temperature in environment and T_i is the excitation energy of electronic state i and become zero for the ground state ($i=1$).

3. Result and discussion

3.1. Potential energy curves, spectroscopic constants and vibrational levels

The 12Λ–S states associated with the lowest dissociation limit (C(^{3}P)+S(^{3}P)) of CS are evaluated at aug-cc-pwCV5Z-DK/MRCI+Q level of theory. The PECs of the 12Λ–S states are presented in Fig. 1. For the sake of visual clarity, we display the singlet Λ–S states and triplet Λ–S states in panels (a) and (b), respectively. And then, we use numerical method to calculate nuclear Schrödinger equations to determine spectroscopic constants. For the convenience of comparison, our calculated spectroscopic constants, including transition energy T_e, vibrational frequencies (ω_e and $\omega_e x_e$), equilibrium distance R_e and dissociation energy D_e, are listed in Table 1, along with the data of previous experimental and theoretical investigations. The spectroscopic constants of electronic states can be served as an effective method to check the precision of electronic structure computation.

As displayed in Fig. 1, the Λ–S states $2^1\Pi$, $2^3\Pi$ and $3^3\Sigma^+$ are qusibound states, and the $A'^1\Sigma^+$ state has shallow potential well with a depth of 0.33 eV. The other 8 Λ–S states are typical bound states, which have potential well deeper than 2.40 eV. In Table 1, one can clearly see that our calculated spectroscopic constants of bound states are generally in good agreement with existing experimental results, as well as the previously available theoretical data. For the $X^1\Sigma^+$ state, the ω_e, $\omega_e x_e$, B_e and R_e are computed to be 1284.2 cm^{-1}, 6.35 cm^{-1}, 0.8179 cm^{-1} and 1.5369 Å, which differ from the latest experimental data by only 1 cm^{-1}, 0.152 cm^{-1}, 0.0021 cm^{-1} and 0.0019 Å. Our calculated dissociation energy of the $X^1\Sigma^+$ state is 7.42 eV, which is only 0.01 eV smaller than experimental value of 7.43 eV.[36] Our calculated spectroscopic constant of the $X^1\Sigma^+$ state has higher accuracy compared with the previously available theoretical results.[24,25] For the first excited state $a^3\Pi$, our calculations present a deep well depth D_e of 3.92 eV located at the R_e of 1.5724 Å. The calculated value of R_e (1.5724 Å) is more close to the experimental value of 1.5691 Å, as compared with previous theoretical data. Our calculated T_e of $a^3\Pi$ (28328 cm^{-1}) agrees well with existing theoretical work of 28173 cm^{-1}, and our calculated T_e of $a^3\Pi$ differs by 1298 cm^{-1} (5%) from previously available experimental data.[18]

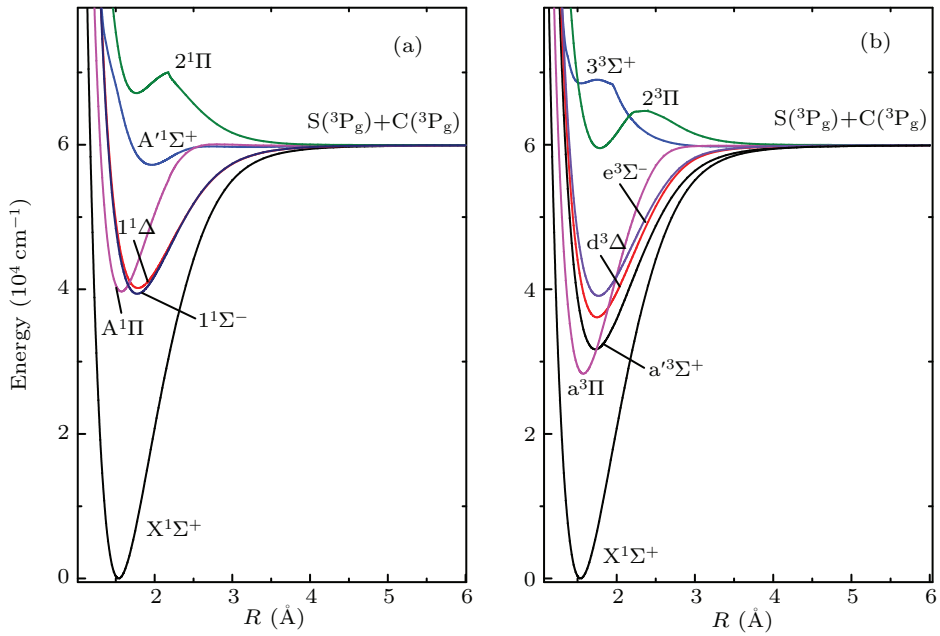


Fig. 1. MRCI+Q potential energy curves for singlet and triplet states of CS along with internuclear distance R.

Table 1. Spectroscopic constants of bound Λ–S states of CS.

State		T_e (cm^{-1})	ω_e (cm^{-1})	$\omega_e x_e$ (cm^{-1})	B_e (cm^{-1})	R_e (Å)	D_e (eV)
$X^1\Sigma^+$	This work	0	1284.2	6.35	0.8179	1.5369	7.42
	Expt.[a]	0	1285.1	6.46	0.8200	1.5349	7.43
	Expt.[b]	0	1285.2	6.502	0.8200	1.535	
	Calc.[c]	0	1284.9	7.83	0.8086	1.543	
	Calc.[d]	0	1273.6	6.36		1.541	
$a^3\Pi$	This work	28328	1125.0	7.47	0.7814	1.5724	3.92
	Expt.[a]	27661	1135.1	7.73	0.7851	1.5687	
	Expt.[b]	27030	1135.4	7.747	0.7848	1.5691	
	Calc.[c]	28173	1135.1	8.96	0.7748	1.587	
$a'^3\Sigma^+$	This work	31709	828.9	5.06	0.6471	1.7279	3.50
	Expt.[a]	31331	830.7	5.04	0.6489	1.725	
	Expt.[b]	30696	829.24	4.943	0.6473	1.728	
	Calc.[c]	31359	836.5	5.85	0.6407	1.741	
$d^3\Delta$	This work	36148	794.2	4.98	0.6327	1.7476	2.95
	Expt.[a]	35675	795.6	4.91	0.6367	1.7420	
	Expt.[b]	35041	796.17	4.966	0.6369	1.742	
	Calc.[c]	35980	798.1	5.72	0.6259	1.757	
$e^3\Sigma^-$	This work	39112	752.9	5.0	0.6186	1.7673	2.58
	Expt.[a]	38683	752	4.7	0.6194	1.766	
	Expt.[b]	38041	752.93	4.955	0.6225	1.762	
	Calc.[c]	38835	750.7	5.4	0.6122	1.778	
$A^1\Pi$	This work	39701	1057.6	10.2	0.7814	1.5725	2.53
	Expt.[a]	38904	1073.4	10.1	0.7800	1.5739	
	Expt.[b]	38255	1077.23	10.639	0.7876	1.566	
	Calc.[c]	39034.8	1062.1	10.95		1.574	
$1^1\Sigma^-$	This work	39406	740.3	5.19	0.6126	1.7759	2.54
$1^1\Delta$	This work	40202	717.8	5.09	0.6062	1.7853	2.45
$A'^1\Sigma^+$	This work	57245	465.7	8.70	0.5016	1.9646	0.33
	Expt.[a]	56505	462.4	7.46	0.5114	1.944	
	Expt.[b]	55864	462.42	7.458	0.5114	1.944	
$2^3\Pi$	This work	59548	744.3	12.81	0.6078	1.7830	

[a]Ref. [36], [b]Ref. [18], [c]Ref. [25], [d]Ref. [24].

In addition, the previous experimental results in Refs. [18, 36] exhibit a relative large difference ($\sim$ 600 cm^{-1}), which may be caused by the experimental error originated from the perturbation of the nearby excited states ($d^3\Delta$, $a'^3\Sigma^+$ and $e^3\Sigma^-$). Similar situations are found in excited states located at the excited energy range of 28000–40000 cm^{-1}, which can also be explained by perturbation caused by a very high density of the excited states. Hence, more accurate spectral studies should be carried out to investigate the perturbations of the excited states. For the first singlet excited state $A^1\Pi$, the dissociation energy D_e is estimated to be 2.53 eV, which can hold 26 vibrational levels. The ω_e, $\omega_e x_e$ and B_e are computed to be 1057.6 cm^{-1}, 10.2 cm^{-1} and 0.7814 cm^{-1}, which are in good accordance with the latest experimental data of 1077.23 cm^{-1}, 10.639 cm^{-1}, and 0.7876 cm^{-1}. The R_e is evaluated to be 1.5725 Å, which is more close to the latest experimental value of 1.566 Å.[18] Our calculated T_e differ by less than 800 cm^{-1} (2%) from the latest measurements.[18] For the second singlet excited state $A'^1\Sigma^+$, the well depth is computed to be 0.33 eV, which can only support 5 vibrational states. Good agreements are achieved for the ω_e, B_e and R_e. In our work, the calculated spectroscopic constants of $A'^1\Sigma^+$ are $\omega_e = 465.7$ cm^{-1}, $B_e = 0.5016$ cm^{-1} and $R_e = 1.9646$ Å, and the ones determined by Ref. [18] are $\omega_e = 462.42$ cm^{-1}, $B_e = 0.5114$ cm^{-1} and $R_e = 1.944$ Å. Our MRCI+Q calculated T_e is 57245 cm^{-1}, which differs by 1381 cm^{-1} (2%) from most recent experimental value of 55864 cm^{-1}.[18] The $\omega_e x_e$ is calculated to be 8.70 cm^{-1}, which is 1.242 cm^{-1} larger than the experimental result of 7.458 cm^{-1}.

In the process of determining spectroscopic constants, the vibrational levels of the ground state and exited states are also obtained. In Tables 2 and 3, the vibrational energy gap between $\Delta v = 1$ are presented for $X^1\Sigma^+$ and $A^1\Pi/A'^1\Sigma^+$ states along with previously available theoretical and experimental data. For the the $X^1\Sigma^+$ state, our calculated vibration levels gap for $v \leq 20$ agree very well with the most recent experimental data,[2] the absolute differences are less than 2 cm^{-1} (0.2%). In comparison with existing theoretical data,[38] our calculated accuracy of vibrational levels has obviously improvement, especially for the $v \geq 2$ vibrational levels. For the $A^1\Pi$ state, the vibration levels gap for $v \leq 4$ are computed to be 1037.6 cm^{-1}, 1016.4 cm^{-1}, 995.9 cm^{-1} and 975.6 cm^{-1}, which is only about $\sim$ 15 cm^{-1} (2%) smaller than the latest experimental results.[20] In addition, our calculated vibration levels gap of $A^1\Pi$ state are closer to experimental data.

Table 2. The vibrational energy gap ($E_v - E_{v-1}$) (in cm^{-1}) for the $X^1\Sigma^+$ state of CS.

	$X^1\Sigma^+$						
	Present	Expt.[a]	Expt.[b]	Expt.[c]	Expt.[d]	Expt.[e]	Calc.[f]
0							
1	1272.2	1272.162085	1272.16214	1272.1690	1272.16	1272.2	1272.2
2	1258.8	1259.191630	1259.19170	1259.1796	1259.19	1259.2	1257.3
3	1245.8	1246.244000	1246.24416	1246.2413	1246.25	1246.2	1242.2
4	1232.9	1233.319135	1233.31939	1233.3188	1233.32	1233.4	1226.9
5	1220.2	1220.416910	1220.41717	1220.4142	1220.41	1220.4	1211.3
6	1207.6	1207.537060	1207.53727	1207.5355	1207.54		
7	1195.2	1194.679260	1194.67942	1194.6754	1194.68		
8	1182.9	1181.843020	1181.84332		1181.85		
9	1170.6	1169.028000	1169.02840		1169.03		
10	1158.0	1156.233400	1156.23450		1156.24		
11	1145.0	1143.458500	1143.46110		1143.48		
12	1131.8	1130.702700	1130.70700				
13	1118.6	1117.965000	1117.97100				
14	1105.8	1105.244300	1105.25500				
15	1093.2	1092.539000	1092.55600				
16	1080.7	1079.850000	1079.87300				
17	1068.2	1067.174000	1067.20000				
18	1055.5	1054.509000	1054.55000				
19	1042.9	1041.857000	1041.90000				
20	1030.3	1029.212000	1029.27000				
21	1017.8	1016.576000					
22	1005.3	1003.945000					
23	992.8	991.319000					
24	980.4	978.695000					
25	967.9	966.069000					
26	955.5	953.440000					

[a]Ref. [2], [b]Ref. [39], [c]Ref. [1], [d]Ref. [18], [e]Ref. [40], [f]Ref. [38].

Table 3. The vibrational energy gap ($E_v - E_{v-1}$) (in cm^{-1}) for the $A^1\Pi$ state of CS.

	$A^1\Pi$						$A'^1\Sigma^+$
	Present	Expt.[a]	Expt.[b]	Expt.[c]	Expt.[d]	Calc.[e]	Present
0					1056.28		
1	1037.6	1035.43	1057.63542	1051.70474	1035.62	1035	448.3
2	1016.4	1048.73	1019.60130	1026.55787		1015	429.3
3	995.9	1017.12		1010.51587		994	407.8
4	975.6	986.00		1006.45262		974	329.7
5	955.5	976.60				950	
6	935.4	949.50					
7	915.2	904.00					
8	894.9	885.00					
9	874.6	871.00					
10	854.2	839.00					
11	833.8						
12	813.1						
13	792.1						
14	770.8						
15	748.9						
16	727.1						
17	706.7						
18	690.7						
19	676.8						
20	649.2						
21	601.1						
22	569.3						
23	531.1						
24	473.8						
25	413.1						
26	318.1						

[a]Ref. [7], [b]Ref. [41], [c]Ref. [20], [d]Ref. [18], [e]Ref. [24].

4. Dipole moments and transition dipole moments

The dipole moments and transition dipole moments of low-lying Λ–S states are computed by employing MRCI wave functions. The dipole moments curves for the singlet Λ–S states and triplet Λ–S states are presented in Figs. 2(a) and 2(b), respectively. As is well known, the vibration of dipole moment reflects the change of electronic configuration for Λ–S state. As displayed in Fig. 2, the extent of variation of dipole moments for $A'^1\Sigma^+$, $2^1\Pi$, $3^3\Sigma^+$ and $2^3\Pi$ are obviously large than that of other 8 Λ–S states. This phenomenon could be explained by the sharp vibration of electronic configuration of $A'^1\Sigma^+$, $2^1\Pi$, $3^3\Sigma^+$ and $2^3\Pi$. As shown in Fig. 1, the $A'^1\Sigma^+$, $2^1\Pi$, $3^3\Sigma^+$ and $2^3\Pi$ are located at high excitation energy range of ≥ 5700 cm^{-1}, which form crossing point with high excited states. The crossing point of $A'^1\Sigma^+$, $2^1\Pi$, $3^3\Sigma^+$ and $2^3\Pi$ cause the sharp change for electronic configurations of those states, hence, the dipole moment curves of $A'^1\Sigma^+$, $2^1\Pi$, $3^3\Sigma^+$ and $2^3\Pi$ change dramatically as compared with that of the other 8 Λ–S states. At the equilibrium distance ($R_e = 1.5369$ Å) of the $X^1\Sigma^+$, the dipole moment is computed to be 0.77 a.u., which agree very well with available experimental data of 0.7704 a.u.[42] Both theoretical and experimental studied indicate the $C^{\delta-}S^{\delta+}$ polarity of the CS molecule. At the equilibrium distance $R_e = 1.5725$ Å, the dipole moment of $A^1\Pi$ is estimated to be 0.29 a.u. As shown in Fig. 2, the dipole moments of all the Λ–S states approach to zero at large internuclear distance, indicating the dissociation products are neutral C and S atoms.

The transition dipole moments (TDMs) of spin-allowed singlet-singlet transition are given in Fig. 3. For convenient of comparing, the previous TDM of $A^1\Pi$–$X^1\Sigma^+$ [24] determined by cc-PVQZ/MRSDCI level of theory are also displayed. As can be seen in Fig. 3, the position of peak of TDM for $A^1\Pi$–$X^1\Sigma^+$ transition in our work and Ref. [24] are well consistent, which are both located at $R = 1.39$ Å. The peak value of TDM of $A^1\Pi$–$X^1\Sigma^+$ transition is 0.304 a.u., which is 0.028 a.u. larger than that in Ref. [24]. The maximum value (0.599 a.u.) of TDM of $A'^1\Sigma^+$–$X^1\Sigma^+$ is located at 1.80 Å.

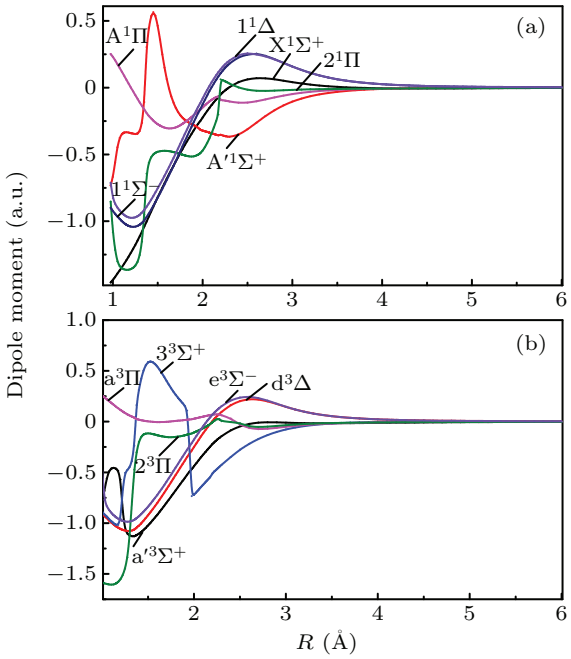


Fig. 2. Dipole moment curves for singlet and triplet states of CS.

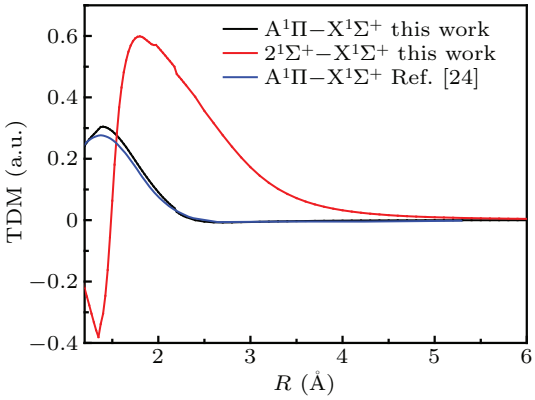


Fig. 3. Transition dipole moment curves of spin-allowed transition of CS.

4.1. Opacity

The opacities of molecules in atmospheric and astrophysical circumstances have been investigated in previous work by using the theoretical method mentioned in Section 2.[43–46] By utilizing the calculated vibration–rotation levels, wavefunctions, DMs and TDMs, the molecular opacity and partition function of CS are computed. The partition function is very important input parameters in spectral analysis and radiative transfer simulation in atmospheric and astrophysical fields. In high density circumstances, the local thermodynamic equilibrium approximation is effective, and the molecular opacity only relies on vibration–rotation levels, degeneracies, TDMs and the gas kinetic temperature T. In our work, the partition functions are determined employing formula (8) via summation over all vibration–rotation levels for the lowest three singlet states. The partition functions of CS versus the temperature T are presented in Fig. 4. As shown in Fig. 4, the total partition functions rapidly increase with the increase of temperature T. When the T increase, the Boltzmann factor $\left(\exp\left(-\frac{T_i hc}{kT}\right)\right)$ grow exponentially, so the partition functions rapidly rise as the temperature rise according to formula (8).

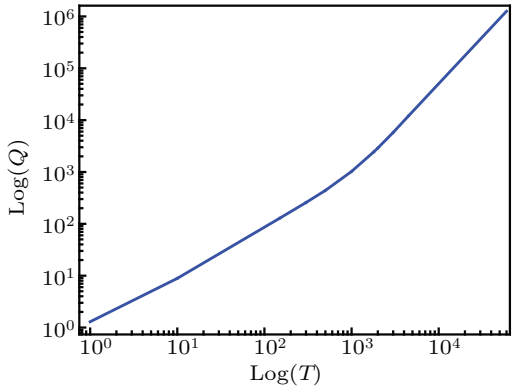


Fig. 4. The total internal partition functions of CS along with the temperature T (in Kelvin).

With the information of partition functions and vibration–rotation states, the molecular opacities for the $X^1\Sigma^+$, $A^1\Pi$ and $A'^1\Sigma^+$ states are obtained from formula (7) at pressure of 100 atms for different temperatures. With the increasing of temperature and growing of density, the dissociation probability of molecule will be raised. However, the dissociation energy of $X^1\Sigma^+$ (7.42 eV) is very large, so the dissociation probability of CS caused by thermal motion in $T = 4500$ K is very small. In addition, the previous investigations also indicate that opacity and absorption spectrum in astrophysical field are mainly originated from molecule.[1,2] The calculated molecular opacities of $X^1\Sigma^+$, $A^1\Pi$ and $A'^1\Sigma^+$ states of CS for the temperatures of 300 K, 1000 K, 1800 K, and 4500 K are displayed in Figs. 5(a)–5(d), respectively. As presented in Fig. 5, the spectra lie in a wide area of wavelengths, which range from UV to far-infrared. In the simulation of spectra, the spectral line is profiled utilizing a Lorentzian function with a width contributed from impact-broadening. As can be observed in Fig. 5(a), there are three electronic bands attributed from three singlet states considered in this work, which associate with $A'^1\Sigma^+$–$X^1\Sigma^+$, $A^1\Pi$–$X^1\Sigma^+$ and $X^1\Sigma^+$–$X^1\Sigma^+$ transitions from left to right, respectively. At low temperature of 300 K/1000 K and a pressure of 100 atms (see Figs. 5(a) and 5(b)), different band systems are distinctly divided from each other. The band systems contributed from $A'^1\Sigma^+$–$X^1\Sigma^+$ and $A^1\Pi$–$X^1\Sigma^+$ transitions appear at nearby 180 nm and 250 nm, which are located in wavelength range of short-wave UV. As for band system of $X^1\Sigma^+$–$X^1\Sigma^+$, there are two typical bands (fundamental vibrational transition and pure rotation transition), and the fundamental vibrational bands of $\Delta v = 1$, 2 and 3 appear around 6.6 μm, 3.4 μm and 2.3 μm, while the pure rotation band of $\Delta v = 0$ locates in wavelength of ≥ 40 μm. It can be seen that the molecular opacities are very small in the 300–1500 nm wavelength range, which form a window area in the visible light (VIS) and near infrared (NIR) region. When the temperature increase (see Figs. 5(c) and 5(d)), the cross section in the

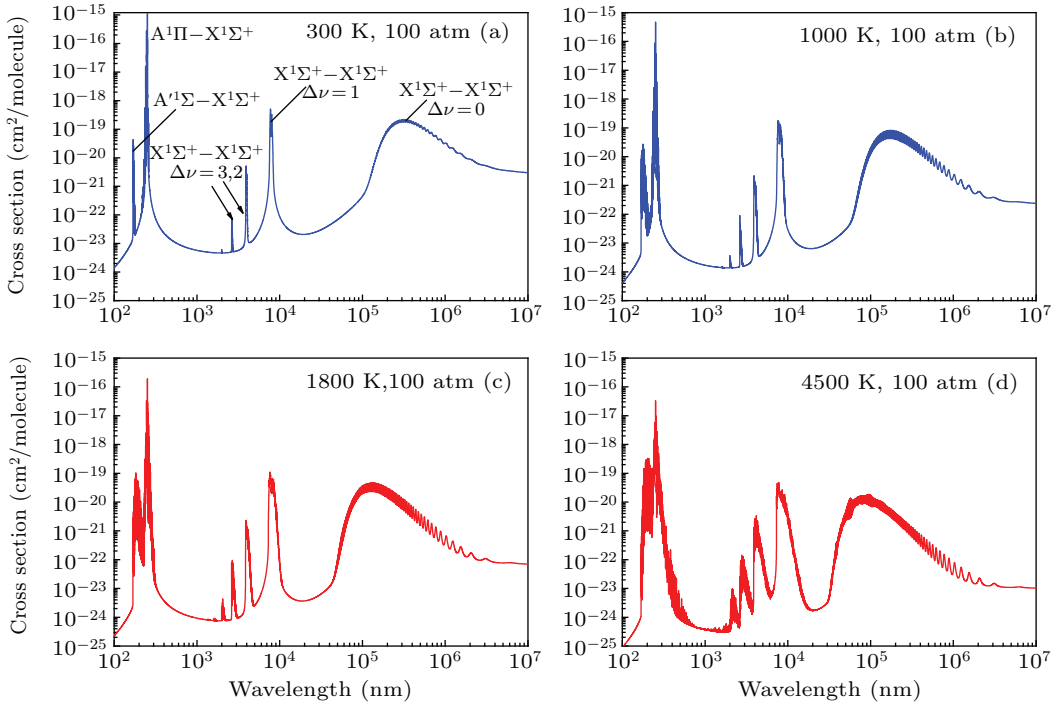


Fig. 5. Opacity of CS generated by vibration–rotation transitions for a pressure of 100 atm and temperatures of $T = 300$ K, 1000 K, 1800 K, and 4500 K.

VIS and NIR window area is growing gradually, and the separation between different fundamental vibrational bands and different electronic bands become blurred, which are originated from the raised population on vibrational excited states and electronic excited state at high temperature. On the other hand, the cross section contributed from pure rotational transition decrease evidently because of the reduced populations on the $X^1\Sigma^+$, while the cross section originated from highly vibrational excited states are enhanced significantly.

5. Conclusions

In this work, accurate PECs of singlet and triplet states correlated with the lowest dissociation limit of CS molecule are computed with high-precision MRCI+Q level of theory. Based on calculated PECs, the spectroscopic constants and vibrational levels are evaluated by using accurate numerical method, which agree with the previous measurement. The opacities for the lowest three singlet states of CS are evaluated at a pressure of 100 atms for the temperatures of 300 K, 1000 K, 1800 K, and 4500 K. At the low temperatures of 300 K and 1000 K, the spectra contributed from electronic transitions ($A'^1\Sigma^+$–$X^1\Sigma^+$ and $A^1\Pi$–$X^1\Sigma^+$) are separated into distinct bands, and different vibrational bands caused by $\Delta v = 0$, 1, 2 and 3 of $X^1\Sigma^+$–$X^1\Sigma^+$ transition are also found. With the increasing of the temperature, the populations on excited states are increased, which cause the superposition of different band transitions. Hence, the band boundaries of cross sections become blurred. This work provides accurate electronic structure and molecular opacity of CS. The present study will shed more light on the calculations of the high-precision molecular structures and opacity.

Acknowledgements

Project supported by the National Natural Science Foundation of China (Grant Nos. 11934004 and 12203106), Fundamental Research Funds in Heilongjiang Province Universities, China (Grant No. 145109127), and the Scientific Research Plan Projects of Heilongjiang Education Department, China (Grant Nos. WNCGQJKF202103 and DWCGQKF202104).

References

[1] Paulose G, Barton E J, Yurchenko S N and Tennyson J 2015 *Mon. Not. R. Astron. Soc.* **454** 1931
[2] Uehara H, Horiai K and Sakamoto Y 2015 *J. Mol. Spectrosc.* **313** 19
[3] Li C L, Deng L H, Zhang J, Qiu X B, Wei J L and Chen Y Q 2013 *J. Mol. Spectrosc.* **284** 29
[4] Sunanda K, Saksena M D, Deo M N, Fujiyama T and Kawaguchi K 2019 *J. Mol. Spectrosc.* **361** 16
[5] Kawaguchi K and Deo M N 2019 *J. Mol. Spectrosc.* **362** 96
[6] Zuo W L, Lv H, Liang H J, Shan S M, Ma R, Yan B and Xu H F 2018 *Chin. Phys. B* **27** 063301
[7] Crawford F H and Shurcliff W A 1934 *Phys. Rev.* **45** 860
[8] Mockler R C and Bird G R 1955 *Phys. Rev.* **98** 1837
[9] Lovas F J and Krupenie PH 1974 *J. Phys. Chem. Ref. Data* **3** 245
[10] Bogey M, Demuynck C and Destombes J L 1981 *Chem. Phys. Lett.* **81** 256
[11] Bogey M, Demuynck C and Destombes J L 1982 *J. Mol. Spectrosc.* **95** 35
[12] Kim E and Yamamoto S 2003 *J. Mol. Spectrosc.* **219** 296
[13] Gottlieb C A, Myers P C and Thaddeus P 2003 *Astrophys.* **588** 655
[14] Todd T R 1977 *J. Mol. Spectrosc.* **66** 162
[15] Winkel R J Jr, Davis S P, Pecyner R and Brault J W 1984 *Can. J. Phys.* **62** 1414

[16] Burkholder J B, Lovejoy E R, Hammer P D and Howard C J 1987 *J. Mol. Spectrosc.* **124** 450
[17] Ram R S, Bernath P F and Davis S P 1995 *J. Mol. Spectrosc.* **173** 146
[18] Bergeman T and Cossart D 1981 *J. Mol. Spectrosc.* **87** 119
[19] Cossart D and Bergeman T 1976 *J. Chem. Phys.* **65** 5462
[20] Mahon C A, Stampanoni A, Luque J and Crosley D R 1997 *J. Mol. Spectrosc.* **183** 18
[21] Dornhöefer G, Hack W and Langel W 1984 *J. Phys. Chem.* **88** 3060
[22] Robbe J M and Schamps J 1976 *J. Chem. Phys.* **65** 5420
[23] Wilson S 1977 *J. Chem. Phys.* **67** 4491
[24] Ornellas F R 1998 *Chem. Phys. Lett.* **296** 25
[25] Hochlaf M, Chambaud G, Rosmus P, Andersen T and Werner H J 1999 *J. Chem. Phys.* **110** 11835
[26] Werner H J, Knowles P J, Knizia G, Manby F R and Schütz M 2012 *Rev. Comput. Mol. Sci.* **2** 242
[27] Jong W A de, Harrison R J and Dixon D A 2001 *J. Chem. Phys.* **114** 48
[28] Dunning T H 1989 *J. Chem. Phys.* **90** 1007
[29] Woon D E and Dunning T H 1993 *J. Chem. Phys.* **98** 1358
[30] Werner H J and Knowles P J 1985 *J. Chem. Phys.* **82** 5053
[31] Knowles P J and Werner H J 1985 *Chem. Phys. Lett.* **115** 259
[32] Werner H J and Knowles P J 1988 *J. Chem. Phys.* **89** 5803
[33] Knowles P J and Werner H 1988 *J Chem. Phys. Lett.* **145** 514
[34] Langhoff S R and Davidson E R 1974 *Int. J Quantum Chem.* **8** 61
[35] Douglas M and Kroll N M 1974 *Ann. Phys.* **82** 89
[36] Huber H P and Herzberg G 1979 *Molecular Spectra and Molecular Structure IV Constants of Diatomic Molecules* (New York: Van Nostrand)
[37] Dulick M, Bauschlicher C W, Burrows A, Sharp C M, Ram R S and Bernath P 2003 *Astrophys. J.* **594** 651
[38] Botschwina P and Sebald P 1985 *J. Mol. Spectrosc.* **110** 1
[39] Coxon J A and Hajigeorgiou G 1992 *Chem. Phys.* **167** 327
[40] Todd T R and Olson W B 1979 *J. Mol. Spectrosc.* **74** 190
[41] Lee L C and Judge D L 1975 *J. Chem. Phys.* **63** 2782
[42] Winnewisser G and Cook R L 1968 *J. Mol. Spectrosc.* **28** 266
[43] Lin X H, Liang G Y, Wang J G, Peng Y G, Shao B, Li R and Wu Y 2019 *Chin. Phys. B* **28** 053101
[44] Liang G Y, Peng Y G, Li R, Wu Y and Wang J G 2020 *Chin. Phys. B* **29** 023101
[45] Liang G Y, Peng Y G, Li R, Wu Y and Wang J G 2020 *Chin. Phys. Lett.* **37** 123101
[46] Zhao S T, Li J, Li R, Yin S and Guo H J 2021 *Chin. Phys. Lett.* **38** 43101